Received: 2 August 2021 | Revised: 23 October 2021 | Accepted: 25 November 2021

DOI: 10.1002/cac2.12244

CANCER COMMUNICATIONS Open Access

ORIGINAL ARTICLE

# Anti-PD-L1/TGF-βR fusion protein (SHR-1701) overcomes disrupted lymphocyte recovery-induced resistance to PD-1/PD-L1 inhibitors in lung cancer

**Bo Cheng**[1,5] | **Kaikai Ding**[3,5] | **Pengxiang Chen**[2] | **Jianxiong Ji**[3,5,8] | **Tao Luo**[3,5] | **Xiaofan Guo**[3,4] | **Wei Qiu**[3,5] | **Chunhong Ma**[7] | **Xue Meng**[1] | **Jian Wang**[3,5,6] | **Jinming Yu**[1] | **Yuan Liu**[2,5]

[1] Department of Radiation Oncology, Shandong Cancer Hospital and Institute, Cheeloo College of Medicine, Shandong University, Jinan, Shandong 250012, P. R. China

[2] Department of Radiation Oncology, Qilu Hospital of Shandong University, Cheeloo College of Medicine, Shandong University, Jinan, Shandong 250012, P. R. China

[3] Department of Neurosurgery, Qilu Hospital of Shandong University, Cheeloo College of Medicine, Shandong University, Jinan, Shandong 250012, P. R. China

[4] Department of Neurology, Loma Linda University Health, Loma Linda, CA 92354, USA

[5] Shandong Key Laboratory of Brain Functional Remodeling, Jinan, Shandong 250012, P. R. China

[6] Department of Biomedicine, University of Bergen, Bergen 5009, Norway

[7] Key Laboratory for Experimental Teratology of Ministry of Education and Department of Immunology, Shandong University School of Medicine, Jinan, Shandong 250012, P. R. China

[8] Department of Neurosurgery, the Second Affiliated Hospital of Zhejiang University School of Medicine, Hangzhou, Zhejiang 310000, P. R. China

**Correspondence**
Yuan Liu, Department of Radiation Oncology, Qilu Hospital of Shandong University, Cheeloo College of Medicine, Shandong University, Jinan 250012, Shandong, P. R. China.
Email: liuyuan9185@163.com
Jinming Yu, Department of Radiation Oncology, Shandong Cancer Hospital and Institute, Cheeloo College of Medicine,

## Abstract

**Background:** Second-generation programmed cell death-protein 1/programmed death-ligand 1 (PD-1/PD-L1) inhibitors, such as bintrafusp alfa (M7824), SHR-1701, and YM101, have been developed to simultaneously block PD-1/PD-L1 and transforming growth factor-beta/transforming growth factor-beta receptor (TGF-β/TGF-βR). Consequently, it is necessary to identify predictive factors of lung cancer patients who are not only resistant to PD-1/PD-

**Abbreviations:** 95% CI, 95% confidence interval; ALC, absolute lymphocyte count; BFA, brefeldin A; BGI, Beijing Genomics Institute; DAB, 3,3'-diaminobenzidine; DDP, cisplatin; DMEM, Dulbecco's modified Eagle's medium; ECACC, European Collection of Authenticated Cell Culture; ECL, enhanced chemiluminescence; EDTA, ethylene diamine tetraacetic acid; ELISA, enzyme-linked immunosorbent assay; FACS, fluorescence activating cell sorting; FBS, fetal bovine serum; FFPE, formalin-fixed paraffin-embedded; G-CSF, granulocyte-colony stimulating factor; GSEA, Gene set enrichment analysis; HR, hazard ratio; IHC, immunohistochemistry; mAb, monoclonal antibody; NLR, neutrophil-to-lymphocyte ratio; NSCLC, non-small cell lung cancer; OS, overall survival; PBMC, peripheral blood mononuclear cell; PD-1, programmed cell death-protein 1; PD-L1, programmed death-ligand 1; PFS, progression-free survival; PLR, platelet-to-lymphocyte ratio; PMA, Phorbol-12-myristate-13-acetate; RNA-seq, RNA sequencing; SEM, standard error of the mean; Teff, effector T cell; TGF-β, transforming growth factor-beta; TGF-βR, transforming growth factor-beta receptor; TMB, tumor mutational burden; TME, tumor microenvironment; TPO, thrombopoietin; Treg, regulatory T cell

Shandong University, Jinan 250012, Shandong, P. R. China.
Email: sdyujinming@163.com

**Funding information**
National Key Research and Development Projects of China, Grant/Award Number: 2018YFC1312201; Academic Promotion Program of Shandong First Medical University, Grant/Award Number: 2019ZL002; National Natural Science Foundation of China, Grant/Award Numbers: 81803096, 81972863, 81627901, 82030082; Natural Science Foundation of Shandong Province, Grant/Award Number: ZR201807080057; Cancer Institute and Hospital, Chinese Academy of Medical Sciences, Grant/Award Number: 2019RU071

L1 inhibitors but also sensitive to bifunctional drugs. The purpose of this study was to search for such predictors.

**Methods:** Multivariable Cox regression was used to study the association between the clinical outcome of treatment with PD-1/PD-L1 inhibitors and lymphocyte recovery after lymphopenia in lung cancer patients. Murine CMT167 lung cancer cells were engineered to express the firefly luciferase gene and implanted orthotopically in the lung of syngeneic mice. Bioluminescence imaging, flow cytometry, and immunohistochemistry were employed to determine response to immunotherapy and function of tumor-infiltrating immune cells.

**Results:** For lung cancer patients treated with anti-PD-1/PD-L1 antibodies, poor lymphocyte recovery was associated with a shorter progression-free survival (PFS; $P < 0.001$), an accumulation of regulatory T cells (Tregs), and an elimination of $CD8^+$ T cells in the peripheral blood. Levels of $CD8^+$ T cells and Treg cells were also imbalanced in the tumors and peripheral immune organs of mice with poor lymphocyte recovery after chemotherapy. Moreover, these mice failed to respond to anti-PD-1 antibodies but remained sensitive to the anti-PD-L1/TGF-$\beta$R fusion protein (SHR-1701). Consistently, SHR-1701 but not anti-PD-1 antibodies, markedly enhanced IFN-$\gamma$ production and Ki-67 expression in peripheral $CD8^+$ T cells from patients with impaired lymphocyte recovery.

**Conclusions:** Lung cancer patients with poor lymphocyte recovery and suffering from persistent lymphopenia after previous chemotherapy are resistant to anti-PD-1/PD-L1 antibodies but might be sensitive to second-generation agents such as SHR-1701.

**KEYWORDS**
anti-PD-L1/TGF-$\beta$R fusion protein, chemotherapy-induced lymphopenia, lung cancer, lymphocyte recovery, PD-1/PD-L1 inhibitor, SHR-1701

## 1 | INTRODUCTION

Lung cancer affects more than 1.8 million people annually and continues to be the most frequent cause of cancer-related death worldwide [1]. The development of programmed cell death protein 1 (PD-1) or its ligand programmed death-ligand 1 (PD-L1) inhibitors constituted a critical breakthrough for lung cancer treatment [2]. Unfortunately, most patients do not have any active response to anti-PD-1/PD-L1 antibodies due to the existence of numerous other immunosuppressive entities in the tumor microenvironment (TME), such as the suppressive cytokine transforming growth factor-beta (TGF-$\beta$), as well as regulatory T cells (Tregs) [2]. Hence, second-generation bifunctional agents such as bintrafusp alfa (M7824), SHR-1701 and YM101 are designed to address this issue, as they can simultaneously block both the PD-1/PD-L1 and TGF-$\beta$/TGF-$\beta$R signaling within the TME. Thus, predictive factors are necessary for the identification of patients who might be resistant to PD-1/PD-L1 inhibitors but remain sensitive to the bifunctional drugs.

M7824 achieved encouraging efficacy and manageable tolerability among non-small cell lung cancer (NSCLC) patients who had previously received platinum treatment in a Phase I clinical trial (NCT02517398). Among the patients with a high PD-L1 expression level, the response to M7824 was as high as 85.7%, significantly higher than that of pembrolizumab [3]. However, a Phase III trial (NCT03631706) for NSCLC using M7824 as first-line treatment was terminated prematurely because M7824 was not superior to pembrolizumab [4] The difference in the results of these two clinical trials suggests that M7824 might be more effective than pembrolizumab in heavily pre-treated patients, but no better than pembrolizumab when used as first-line therapy.

Platinum-based chemotherapy is often accompanied by neutropenia, thrombocytopenia, and lymphopenia. The rapid repopulation of neutrophils and platelets can be

easily achieved by the administration of granulocyte-colony stimulating factor (G-CSF) and thrombopoietin (TPO). However, there is no specific drug for lymphopenia. Patients with lymphopenia after chemotherapy are further classified as "rapid recovery" or "poor recovery". Rapid lymphocyte recovery has been regarded as a potential marker of prolonged survival in patients with advanced thoracic cancers and locally advanced pancreatic cancer [5, 6]. It has been reported that 57% of cancer patients with lymphopenia achieved rapid recovery, even leading to the extensive proliferation of effector T (Teff) cells. However, among the other 43% of patients, the lymphopenia was severe and unexpectedly long-lasting [7, 8], resulting in an elevated neutrophil-to-lymphocyte ratio (NLR) and platelet-to-lymphocyte ratio (PLR). Since high NLR and PLR are prognostic markers strongly correlated with the poor response of patients receiving PD-1/PD-L1 inhibitors [9, 10], then poor lymphocyte recovery after first-line chemotherapy might cause the resistance to anti-PD-1/PD-L1 antibodies.

Lymphopenia can be quickly resolved by active T cell proliferation in tumor bearers with rapid lymphocyte recovery [11, 12]. Nevertheless, homeostatic proliferation is disrupted by chemotherapy in nearly half of cancer patients and the mechanism for this remains unclear. TGF-$\beta$ plays an important role in many immune cell lineages. TGF-$\beta$ absence leads to a significant proliferation of Teff cells after transient lymphopenia in non-tumor bearers. [13]. However, its role in regulating chemotherapy-related lymphopenia in patients with tumors has not been described.

To our knowledge, no prior study has examined the association between lymphocyte recovery and the clinical outcome of cancer patients who received PD-1/PD-L1 blockade therapy. Moreover, no predictive factors have been reported to help in the identification of patients specifically sensitive to second-generation bifunctional drugs. Therefore, this study aimed to investigate the clinical role of lymphocyte recovery in predicting the responses to the second generation of PD-1/PD-L1 inhibitors in lung cancer.

## 2 | MATERIALS AND METHODS

### 2.1 | Patients

Based on published literature [14], satisfied/rapid lymphocyte recovery was defined as 3 consecutive days in which absolute lymphocyte count (ALC) was $\geq 1000/\mu$L within 3 weeks following previous anti-tumor treatments. In contrast, the definition of poor/impaired/destroyed lymphocyte recovery was that the ALC could not reach 1000/$\mu$L even beyond 3 weeks after previous anti-tumor treatments and remained to be $< 1000/\mu$L when the immunotherapy started.

A retrospective analysis of 205 lung cancer patients who received PD-1/PD-L1 blockade immunotherapy at Qilu Hospital of Shandong University (Jinan, Shandong, China) from June 2017 to June 2021 was performed. Clinical data was collected from medical records. Inclusion criteria were: histologically or cytologically confirmed lung cancer (stage II/III/IV, including local, regional and distant recurrence), had not been operated on before, received immunotherapy in the first or later lines, and with follow-ups every 3 months after immunotherapy, including imaging examination and hematological tests. Patients had no previous history of pulmonary or systematic diseases. Previous or concurrent treatment (cytotoxic chemotherapy, biological therapy, and/or radiation) was allowed. Patients with poor performance status (Karnofsky score $< 60$) were excluded.

Peripheral blood samples were obtained for in vitro studies from 34 patients with lung cancer with satisfied or poor lymphocyte recovery. Patients' inclusion criteria were: age $\geq 18$ years old, pathologically diagnosed with lung cancer, adequate hematological function and availability of peripheral blood samples. Patients with severe co-morbidities or autoimmune diseases were excluded.

The study protocol was approved by the Medical Ethical Committee of Qilu Hospital affiliated to Shandong University (permit number: KYLL-2019-2-004). The blood samples were obtained with written informed consent from each patient.

### 2.2 | Cell culture

The mouse lung cancer cell line CMT167 was obtained from the European Collection of Authenticated Cell Cultures (ECACC) and cultured in Dulbecco's modified Eagle's medium (DMEM; Life Technologies, Carlsbad, California, USA), containing 10% (v/v) fetal bovine serum (FBS; Life Technologies) at 37°C in a humidified atmosphere with 20% $O_2$ and 5% $CO_2$.

### 2.3 | Lentiviral transfection

CMT167 cells were transfected with firefly luciferase lentivirus (GeneChem, Shanghai, China) following the manufacturer's protocol. Briefly, CMT167 cells were incubated with viral stocks supplemented with 4 $\mu$g/mL Polybrene (#107689, Sigma-Aldrich, St Louis, MO, USA) for 6 h and then supplied with fresh medium. The transduced cells were then supplied with 2 $\mu$g/mL puromycin (#P8833, Sigma-Aldrich) 2 days after transduction to clear the

non-transduced cells. Ten days after transduction, isolation of cell clones was performed.

## 2.4 | Animal study

Animal studies were approved by Institutional Animal Care and Use Committee of Qilu Hospital affiliated to Shandong University (permit number: DWLL-2020-045). The mice were bred in our air-conditioned animal facility and housed with a 12/12 hr light/dark cycle and with ad libitum access to food and water. The housing, breeding, and animal experiments were in accordance with the recommendations in the Guide for the Care and Use of Laboratory Animals of the National Institutes of Health. In the survival study, the animals were observed daily. Humane endpoints were used during this study: moribund were humanely euthanized. We used two criteria to identify the moribund animals based on our animal use protocol: 1) mouse has difficulty breathing, eating, or drinking; 2) a mouse loses ≥ 15% body weight in 4 days. Euthanasia is performed after deep anesthesia in order to alleviate suffering.

Sample sizes of animal studies were determined using a power analysis. Luciferase-expressing CMT167 cell lines ($5 * 10^5$ cells in 40 $\mu$L PBS) were injected through the chest wall into the lung of C57BL/6 (5-week-old; SPF Biotechnology Co., Ltd, Beijing, China) female mice on day 0. Tumor growth was examined at 5, 10, and 15 days after inoculation via bioluminescence imaging (IVIS spectrum in vivo imaging system, PerkinElmer, Hopkinton, MA, USA). On day 5, mice were randomly assigned to each treatment group. For cisplatin (DDP, #H20023460, Qilu Pharmaceutical, Jinan, Shandong, China) groups, DDP was intraperitoneally (i.p.) administered for four days (from day 5 to day 8) at a dose of 4 mg/kg daily. For the anti-PD-1 group, an anti-mouse PD-1 monoclonal antibody (mAb, 200 $\mu$g/mouse/day; #BE0146, BioXcell, West Lebanon, NH, USA) was administered i.p. on days 5, 8, 11 and 14 (every 3 days). For the concomitant therapy group, an anti-PD-1 mAb was administered i.p. every third day, starting at day 5 with DDP together. For the sequential chemoimmunotherapy group, DDP was given on days 5-8, followed by anti-PD-1 mAb administered starting on day 8. For the dual immunotherapy and SHR-1701 groups, anti-TGF-$\beta$ (300 $\mu$g/mouse/day; #BE0057, BioXcell), anti-PD-1 (200 $\mu$g/mouse/day), as well as SHR-1701 (200 $\mu$g/mouse/day) mAbs were administered i.p. every third day from day 8 to day 14. The control group was injected with an equal volume of PBS or isotype on each injection day. SHR-1701 is not currently commercially available and was a kind gift from Jiangsu Hengrui Medicine Co., Ltd (Shanghai, China).

## 2.5 | Flow cytometry

A total of 5 mL peripheral blood was collected from lung cancer patients ≥ 3 weeks after the last cycle of chemotherapy. The flow cytometry analysis of peripheral lymphocytes was conducted in all fresh heparinized peripheral blood extracted from lung cancer patients ($n = 34$), with matching clinical data obtained from the Department of Radiation Oncology at Qilu Hospital of Shandong University. Informed written consent was obtained from all patients.

Blood samples were processed within 6 h. Peripheral blood mononuclear cells were prepared by centrifugation with Ficoll-Paque Plus (Amersham Biosciences, Piscataway, NJ, USA). Fresh PBMCs were isolated and stained with a master mix of Abs at 4°C for 30 min. The markers CD3 (1:20; #300326, Biolegend, San Diego, CA, USA) and CD8 (1:20; #344704, Biolegend) were used to discern $CD8^+$ T cells. Treg cells were retrieved by gating for the high expression of CD4 (1:20; #357404, Biolegend) and CD25 (1:20; #302610, Biolegend).

Single-cell suspensions of the harvested mouse spleens and tumors were prepared and stained with a cocktail of Abs against the following surface markers: CD3 (1:20; #100205, #100218, Biolegend), CD8 (1:20; #237367, #ab237368, Abcam, Cambridge, MA, USA), CD4 (1:20; #100406, Biolegend), PD-1 (1:20; #135210, Biolegend), GITR (1:20; #126312, Biolegend), and CD69 (1:20; #104508, Biolegend). Permeabilization was performed using the Fixation/Permeabilization Concentrate and Diluent (1:25; #562574, BD, Franklin Lakes, NJ, USA), and cells were subsequently stained intracellularly with Foxp3 (1:20; #563902, BD), Ki-67 (1:20; #561283, BD), and IFN-$\gamma$ (1:20; #505808, Biolegend).

Flow analysis were performed on a BD FACS Aria III cytometer equipped with a 405 nm laser, a 488 nm laser, and a 635 nm laser. Cells should be filtered through nylon mesh. FlowJo software (version 8.7, TreeStar, Ashland, OR) for analysis of acquired raw data.

## 2.6 | In vitro cell stimulation

After 24 h of incubation in lymphocyte medium KBM 551 (#88-551-CM, Corning, New York, USA) supplemented with 10% FBS and 300 IU/mL murine IL-2 (#212-12-100, PeproTech, Rocky Hill, NJ, USA), the single-cell suspensions (PBMCs, splenic cells or tumor infiltrating lymphocytes) were transferred to 96-well plates coated with 5 $\mu$g/mL CD3 (#100360, Biolegend) and 2 $\mu$g/mL CD28 (#102131, Biolegend) for 48 h. The cells were treated for 4∼6 h with 5 $\mu$g/mL brefeldin A (BFA, #420601, Biolegend) before lymphocytes were harvested for flow cytometry.

## 2.7 | In vitro drug effectiveness assay

To verify that SHR-1701 blocked the TGF-$\beta$R in mouse tumor cells, CMT167 cells were treated with SHR-1701 (10 $\mu$g/mL) or control IgG at 37°C for 40 min. In order to ensure that TGF-$\beta$R was indeed blocked by SHR-1701 in an original activated state, the cells were incubated with recombinant mouse TGF-$\beta$1 (8 ng/mL; #763104, Biolegend) for 40 min with or without SHR-1701. Similarly, for the sake of determinizing the activation status of the Akt signaling pathway in tumor cells, CMT167 cells incubated with SHR-1701 or control IgG for 40 min were transferred to a plate coated with recombinant mouse PD-L1-Fc chimera (5 $\mu$g/mL; #758206, Biolegend). The proteins were purified after 24 h followed by western blotting analysis.

To verify that SHR-1701 rescued the anti-tumor function of $CD8^+$ T cells in lung cancer patients, PBMCs extracted from patients were pretreated with 10 $\mu$g/mL SHR-1701, 10 $\mu$g/mL anti-PD-1 Abs (#AF1086, R&D systems, Minneapolis, Minnesota, USA) or 1 $\mu$mol/L TGF-$\beta$R inhibitors (#S1476, Selleck, Houston, Texas, USA) for 3h at 37°C.Then PBMCs were treated with Phorbol-12-myristate-13-acetate (PMA, 10 ng/mL; #P1585, Sigma-Aldrich) and ionomycin (1 $\mu$g/mL; #HY-13434, MedChemExpress, Princeton, NJ, USA) for 4 h before the $CD8^+$ and $CD4^+$ T cell were isolated and collected for further examinations.

## 2.8 | Western blotting

For western blotting, the primary antibodies against the following proteins were used: pSmad2 (1:1000; #18338, Cell Signaling Technology, Beverly, MA, USA), Smad2 (1:1000; #5339, Cell Signaling Technology), pAkt (1:1000; #4060, Cell Signaling Technology), Akt (1:1000; #4691, Cell Signaling Technology), pErk (1:1000; #9101, Cell Signaling Technology), Erk (1:1000; #4695, Cell Signaling Technology), TGF-$\beta$R (1:1000; #ab184948, Abcam), Vinculin (1:1000; #ab129002, Abcam), GAPDH (1:1000; #ab9485, Abcam), Foxp3 (1:1000; #320202, Biolegend). Western blotting was performed as previous reported [15]. Briefly, cells were lysed in RIPA lysis buffer (#89901, Thermo Fisher Scientific, Waltham, MA, USA). Up to 50ng/ml proteins were resolved by SDS-polyacrylamide gels (#NP0323BOX, Thermo Fisher Scientific) and transferred to polyvinylidene fluoride membranes (#3010040001, Solarbio, Beijing, China). Primary antibodies and secondary horseradish peroxidase-conjugated antibodies (#ZB-2301, #ZB-2305, ZSGB-BIO, Beijing, China) were used for the assay. The proteins were detected using an enhanced chemiluminescence (ECL, #34096, Thermo Fisher Scientific) detection system.

## 2.9 | Flow sorting and RNA sequencing (RNA-seq)

Tumor-infiltrating mononuclear cells were stained with appropriate dilutions of anti-CD3 (1:20; #100218, Biolegend) + anti-CD8 (1:20; #155005, Biolegend)/anti-CD4 (1:20; #100406, Biolegend) + anti-CD25 (1:20; #162103, Biolegend) Abs at room temperature. The stained cells were resuspended in a final volume of 500 $\mu$L in saline solution and subsequently filtered into polypropylene fluorescence activating cell sorting (FACS) tubes. 1* $10^6$ cells were sorted using a BD FACS Aria III into 1.5 mL tubes prefilled with 1mL saline solution. After sorting the $CD3^+CD8^+$ T cells and $CD4^+CD25^+$ Treg cells, the total RNA was isolated for RNA-seq analysis. Based on the BGISEQ-2000 platform (Beijing Genomics Institute, Beijing, China), construction and sequencing of the cDNA library were conducted at the Beijing Genomics Institute (BGI; Beijing, China). The expression of these clean reads was summarized using software developed by BGI, and Immunesigdb from MSigDB was used to annotate, analyze, and enrich the gene set.

Gene set enrichment analysis (GSEA) was performed using pre-ranked gene lists. GSEA Preranked version 6.0.12 was used with default parameters and data were exported and graphed in GraphPad Prism version 8 (La Jolla, CA, USA).

## 2.10 | Immunohistochemistry (IHC)

Briefly, 4-$\mu$m formalin-fixed paraffin-embedded (FFPE) sections were deparaffinized, rehydrated and incubated in Ethylene Diamine Tetraacetic Acid (EDTA, #C1034, Solarbio) at 95°C for 20 min to retrieve the antigen. IHC assays were performed using the SPlink Detection Kit (#SP-9000, ZSJQ-Bio, Beijing, China) according to the manufacturer's instructions. Briefly, after treatment with endogenous peroxidase blocking solution at 37°C for 30 minutes, tissues were blocked with goat serum for 30 minutes and incubated with primary antibodies overnight. Primary antibodies were diluted according to the instructions. Sections were then incubated with goat anti-mouse/rabbit IgG and horseradish peroxidase enzyme-labeled streptomycin in order. Finally, sections were developed with 3,3'-diaminobenzidine tetrahydrochloride (DAB, #ZLI-9017, ZSJQ-Bio). Hematoxylin (#ZLI-9610, ZSJQ-Bio) was used for counterstaining. The following primary Abs were used: CD8 (1:2000; #ab209775, Abcam), Foxp3 (1:1000; #ab215206, Abcam), IL-2 (1:500; #ab227834, Abcam), TGF-$\beta$ (1:1000; #ab229856, Abcam). IHC images were evaluated by two blinded pathologists, with the intensity of staining scored from 0 to 3, with 0 (no staining),

1 (light yellow, weakly positive), 2 (yellowish-brown, moderately positive), and 3 (brown, strongly positive). The percentage of positive cells was also scored using a scale of 0-3: 0 (0%), 1 (1%-33%), 2 (34%-66%), and 3 (67%-100%). The intensity and percentage scores were added to obtain a final total score, with low expression defined as a total score of 0-3, and high expression defined as 4-6.

### 2.11 | Enzyme-linked immunosorbent assay (ELISA)

Serum levels of IL-2 and TGF-$\beta$ were measured by commercial ELISA kits (#SEA073Hu for IL-2, #SEA124Hu for TGF-$\beta$, Cloud-Clone, Wuhan, Hubei, China). A total of 100 $\mu$L serum was placed into a 96-well plate coated with an Ab specific to the marker and incubated at 37°C for 60 min. Then, the diluted biotin-conjugated Ab (100 $\mu$L) was added to the wells and incubated at 37°C for 60 min. Subsequently, Avidin-HRP conjugate (100 $\mu$L) was supplemented into the wells at 37°C for 30 min, then washed before reaction with 3,3',5,5'-tetramethylbenzidine (90 $\mu$L) as the chromogenic reagent occurred in the dark for 10-20 min. The reaction was terminated with a sulfuric acid solution (60 $\mu$L) and the absorbance was measured using EnSight Multimode Plate Reader (Perkin Elmer, Boston, MA, USA) at 450 nm.

### 2.12 | Statistical analysis

The therapeutic response to anti-PD-1/PD-L1 antibodies and the progression-free survival (PFS) values of 205 patients were retrospectively collected. The primary endpoint was PFS, which was defined as the time from the start of immunotherapy to the first disease progression. The secondary endpoint was overall survival (OS), which was defined as the time from the start of immunotherapy to death as a result of any cause. Besides, multiple factors, including age, sex, TNM stage, histological subtype, the number of prior treatment lines, radiotherapy, chemotherapy, antiangiogenetic therapy, toxicities and lymphocyte recovery were statistically analyzed. The variable of lymphocyte recovery (0 for poor lymphocyte recovery; 1 for satisfied lymphocyte recovery) was dichotomous. Multivariable Cox regression analysis was used to study the relationship between lymphocyte recovery and PFS. Baseline variables that were considered clinically relevant were entered into multivariate Cox regression model. Variables for inclusion were carefully chosen, given the number of events available, to ensure parsimony of the final model. Hazard ratio (HR) and 95% confidence interval (CI) were used to draw forest map. Kaplan-Meier survival curve was drawn directly using the SPSS software (Version 23; Chicago, IL, USA). The median follow-up, median survival and *P*-values of the survival curve were also calculated using the Kaplan-Meier analysis. All statistical tests were two-sided, and $P < 0.050$ was termed as significant.

For basic experiments, the data were expressed as mean ± standard error of the mean (SEM). The unpaired two-tailed Student's t-test was used to compare differences between two groups. Multiple comparisons were performed with one-way ANOVA using Dunnett's multiple comparisons test. Statistical analysis was conducted using GraphPad Prism (Version 8.0). $P < 0.050$ was considered statistically significant for all the two-sided tests.

## 3 | RESULTS

### 3.1 | Lymphocyte recovery is associated with immunotherapy response in lung cancer

The use of peripheral NLR and PLR as prognostic predictors of immunotherapy outcomes in lung cancer patients has been previously reported [9, 10]. In this study, NLRs and PLRs were dynamically monitored during chemotherapy in locally advanced or advanced lung cancer patients who would receive the subsequent immunotherapy. In patients with poor lymphocyte recovery, their ALC dropped sharply and did not recover for at least 3 weeks, even after the patient had begun immunotherapy (Figures 1A and 1B). However, neutrophils and platelets were maintained at normal levels due to conventional medications, such as G-CSF and TPO (Figures 1A and 1B). Thus, chemotherapy caused a dramatic and lasting increase in both peripheral NLR and PLR in these patients, indicating a poor response to subsequent immunotherapy (Figures 1C and 1D).

Therefore, we investigated whether lymphocyte recovery could independently predict the response to PD-1/PD-L1 inhibitors.

A total of 205 lung cancer patients who received immunotherapy in Qilu Hospital were included in the retrospective study. The detailed inclusion criteria are shown in "Materials and Methods" section. As shown in Table 1, each baseline characteristic was equally distributed among the enrolled 205 patients. Then, we analyzed the PFS of patients with or without satisfied lymphocyte recovery using Kaplan-Meier survival analysis and multivariable Cox regression analysis. The results showed that the median follow-up was 180 days (95%CI = 147-213). The median PFS was 17 days for patients with poor lymphocyte recovery and was significantly shorter than that for patients with satisfied lymphocyte recovery [17.000 days

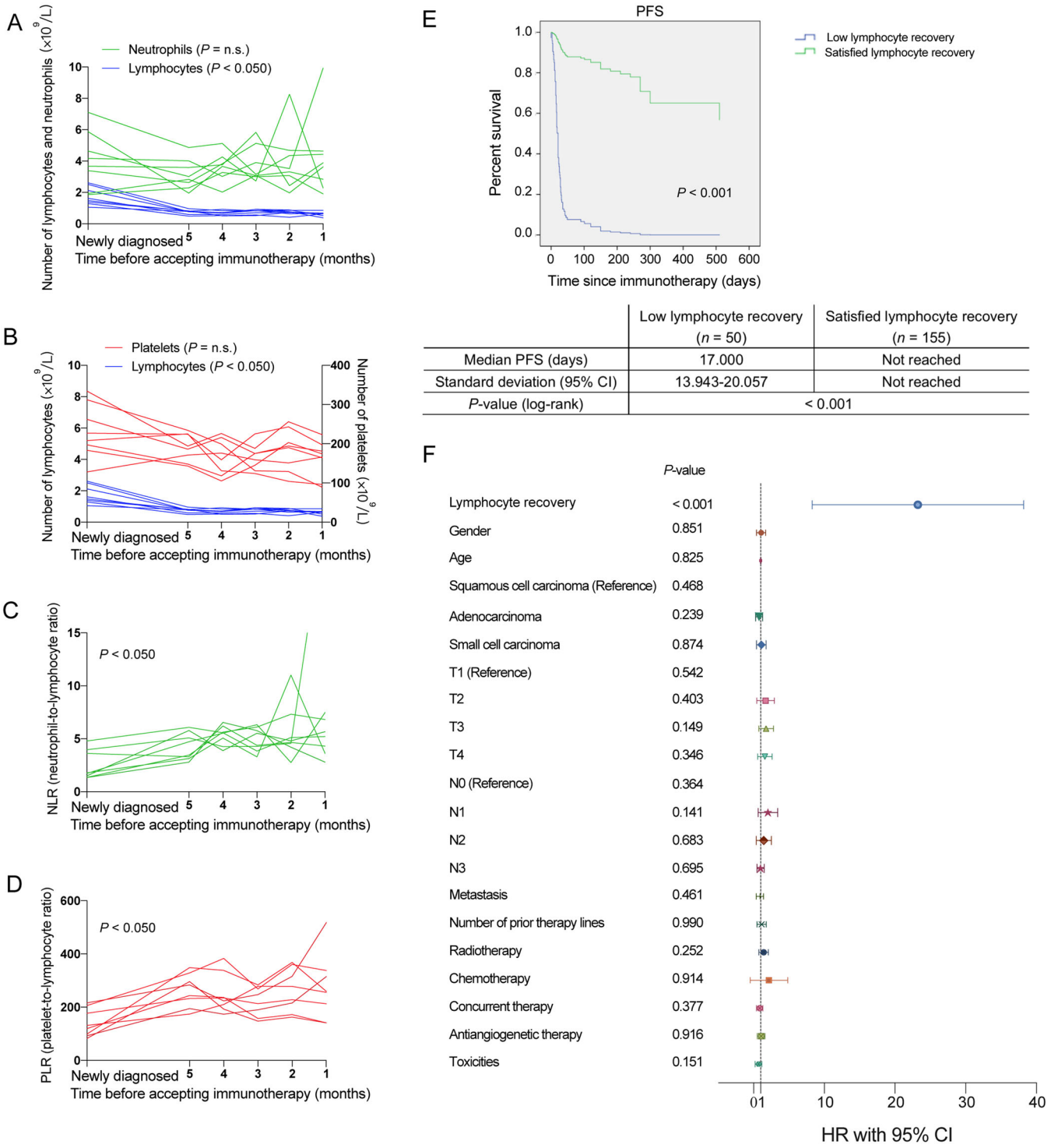


| | Low lymphocyte recovery ($n$ = 50) | Satisfied lymphocyte recovery ($n$ = 155) |
|---|---|---|
| Median PFS (days) | 17.000 | Not reached |
| Standard deviation (95% CI) | 13.943-20.057 | Not reached |
| $P$-value (log-rank) | < 0.001 | |

**FIGURE 1** Subgroup analysis of the relationship between lymphocyte recovery and progression-free survival (PFS) in patients with lung cancer receiving immunotherapy. **(A-D)** The number of lymphocytes (A and B), neutrophils (A), platelets (B), NLR (C), and PLR (D) from eight patients over time before receiving immunotherapy. **(E)** PFS curve of patients with low or satisfied lymphocyte recovery. **(F)** Forest plots of PFS by patient subgroups: poor lymphocyte recovery versus satisfied lymphocyte recovery. A-D: $n = 8$; E-F: $n = 205$. One-way ANOVA analysis was used in A-D. Cox regression analysis, Kaplan-Meier survival estimate, and log-rank tests were used in E and F.

**Abbreviations**: NLR, neutrophil-to-lymphocyte ratio; PLR, platelet-to-lymphocyte ratio; PFS, progression-free survival; HR, hazard ratio; CI, confidence interval; n.s., not significant

**TABLE 1** Clinical characteristics of 205 patients with lung cancer

| Clinical characteristics | | Total (%) | Satisfied lymphocyte recovery | | *P*-value |
|---|---|---|---|---|---|
| | | | With | Without | |
| Age category | | | | | |
| | < 65 | 96 (46.8) | 69 | 27 | 0.825 |
| | ≥ 65 | 109 (53.2) | 86 | 23 | |
| Gender (cases [%]) | | | | | |
| | Female | 164 (80.0) | 28 | 13 | 0.851 |
| | Male | 41 (20.0) | 127 | 37 | |
| Histology (cases [%]) | | | | | |
| | Squamous cell carcinoma | 73 (35.6) | 58 | 15 | 0.468 |
| | Adenocarcinoma | 84 (41.0) | 68 | 16 | 0.239 |
| | Small cell carcinoma | 48 (23.4) | 29 | 19 | 0.874 |
| Number of prior therapy lines (cases [%]) | | | | | |
| | 1 | 85 (41.5) | 78 | 7 | 0.990 |
| | > 1 | 120 (58.5) | 77 | 43 | |
| T stage (cases [%]) | | | | | |
| | T1 | 38 (18.5) | 33 | 5 | 0.542 |
| | T2 | 66 (32.2) | 45 | 21 | 0.403 |
| | T3 | 38 (18.5) | 30 | 8 | 0.149 |
| | T4 | 63 (30.7) | 47 | 16 | 0.346 |
| N stage (cases [%]) | | | | | |
| | N0 | 31 (15.1) | 26 | 5 | 0.364 |
| | N1 | 19 (9.3) | 13 | 6 | 0.141 |
| | N2 | 77 (37.6) | 65 | 12 | 0.683 |
| | N3 | 78 (38.0) | 51 | 27 | 0.695 |
| M stage (cases [%]) | | | | | |
| | M0 | 78 (38.0) | 67 | 11 | 0.461 |
| | M1 | 127 (62.0) | 88 | 39 | |
| Radiotherapy (cases [%]) | | | | | |
| | No | 122 (59.5) | 99 | 23 | 0.252 |
| | Yes | 83 (40.5) | 56 | 27 | |
| Chemotherapy (cases [%]) | | | | | |
| | No | 13 (6.3) | 13 | 0 | 0.914 |
| | Yes | 192 (93.7) | 142 | 50 | |
| Concurrent chemotherapy (cases [%]) | | | | | |
| | No | 57 (27.8) | 43 | 14 | 0.377 |
| | Yes | 148 (72.2) | 112 | 36 | |
| Previous/Concurrent antiangiogenetic therapy (cases [%]) | | | | | |
| | No | 126 (61.5) | 102 | 24 | 0.916 |
| | Yes | 79 (38.5) | 53 | 26 | |
| Toxicities (cases [%]) | | | | | |
| | No | 185 (90.2) | 139 | 46 | 0.151 |
| | Yes | 20 (9.8) | 16 | 4 | |
| Lymphocyte recovery (cases [%]) | | | | | |
| | With | 50 (24.4) | | | <0.001 |
| | Without | 155 (75.6) | | | |

(95%CI = 13.943-20.057) versus median PFS not reached, respectively, $P < 0.001$, Figure 1E]. However, the median overall survival in both groups was not reached. Subsequently, clinically relevant factors, including age, sex, TNM stage, histological subtype, the number of prior treatment lines, radiotherapy, chemotherapy, antiangiogenetic therapy, toxicities and lymphocyte recovery were entered into the multivariate Cox regression analysis. The results showed that PFS was not related to age, sex, histology, clinical-stage, chemotherapy, radiotherapy or antiangiogenic therapy, but to lymphocyte recovery (HR = 20.024, 95%CI = 10.141-39.539, $P < 0.001$, Figure 1F).

## 3.2 | Changes of circulating T cell subsets in lung cancer patients with poor lymphocyte recovery

PBMCs were isolated and the circulating T cell subsets were analyzed. Blood samples were collected from 34 lung cancer patients and the phenotypic expression of PBMCs was evaluated by flow cytometry. Of the 34 patients, 16 (47%) suffered from persistent lymphopenia for more than 3 weeks and were regarded as having impaired lymphocyte recovery, while the other 18 (53%) rapidly recovered in less than 3 weeks. Compared to patients with rapid recovery, patients with persistent lymphopenia exhibited a significantly higher proportion of $CD3^+CD4^+CD25^+$ Tregs ($P < 0.001$, Figure 2A), with no difference in the proportion of $CD3^+CD8^+$ T cells (Figure 2B). Thus, the $CD8^+$ T cell/Treg ratio was significantly decreased in patients with poor lymphocyte recovery ($P < 0.010$, Figure 2C).

## 3.3 | The $CD8^+$ T to Treg cell ratios in the thymus, spleen and TME are reduced in orthotopic lung cancer mouse model with impaired lymphocyte recovery

We then set out to extend these clinical observations of peripheral $CD8^+$ T cell/Treg down-regulation using mouse models to further explore lymphopenia-related changes in TME. An orthotopic model was utilized, in which CMT167 murine lung cancer cells were transplanted into the lungs of syngeneic C57BL/6 mice (Figure S1A). Many factors can impair the lymphocyte recovery of lung cancer patients, such as age, underlying diseases, surgery, and various antitumor treatments. Of all the causes, chemotherapy is the most common one, thus, we chose DDP to build the model as a representation . Our preliminary data demonstrated that lymphocyte recovery could be disrupted when the mice are injected with 4 mg/kg of DDP for 4 days. Flow cytometry of circulating blood leukocytes revealed that the total lymphocyte numbers were significantly reduced after DDP treatment ($P < 0.001$, Figure 2D) but there was no significant difference in the proportion of peripheral $CD3^+CD8^+$ T cells (Figure 2E). Surprisingly, in contrast to the reduced absolute number of circulating $CD8^+$ T cells (Figure 2E), the absolute number of $CD4^+CD25^+$ Tregs greatly increased ($P < 0.001$, Figure 2F), thereby shifting the $CD8^+$ T cell/Treg ratio ($P < 0.050$, Figure 2G). Spleens and thymus shrank in DDP-treated mice (Figure S1B) and pathological structures were also detected. In DDP-treated animals, the cortical area declined in thickness, while areas of the connective and glandular tissue of the thymus expanded in comparison to the control group. Splenic corpuscles were also damaged or absent (Figure S1C).

In addition, mice with DDP-induced lymphopenia harbored more $Foxp3^+$ Treg cells but fewer $CD8^+$ Teff cells in the thymus, spleen, and tumor, which was confirmed by IHC (Figure 3A-F). Thus, the ratios of $CD8^+$ T/Treg cells in the thymus, spleen, and tumor were also lowered by DDP (Figure 3G-I). Additionally, the tumor $CD4^+$ T cells were sorted, and total RNA was isolated for RNA-seq analysis. Gene Set Enrichment Analysis (GSE7582, and GSE20366) revealed that DDP treatment was significantly related to Treg differentiation in TME ($P < 0.010$, Figures 3J and 3K).

## 3.4 | The activation of peripheral, splenic, and tumor-infiltrating $CD8^+$ T cells (TILs) is suppressed in mice with disrupted lymphocyte recovery

To assess the activation status of $CD8^+$ T cells, intracellular Ki-67 was examined, as it is a cell-cycle regulation marker expressed in proliferating mammalian cells [16]. Increase in $Ki\text{-}67^+$ T cells in the peripheral blood is an indicator for NSCLC patients with $CD8^+$ T cell responses triggered by PD-1-targeted therapy [17]. Consistent with these previous reports, peripheral, splenic as well as $CD8^+$ TILs of mice with poor lymphocyte recovery presented a significantly lower frequency of $Ki\text{-}67^+$ cells than control (Figure 4A-C). In addition, after CD3/CD28 co-stimulation, the frequency of tumor-infiltrating and splenic $Ki\text{-}67^+$ $CD8^+$ T cells were further elevated in control mice while there was no response to CD3/CD28 co-stimulation in DDP-treated mice (Figure 4B and 4C). Similar expression of PD-1 protein was found in $CD8^+$ T cells in both groups (Figure 4D), with DDP-treated mice having a higher frequency of $PD\text{-}1^+$ Treg cells than control subjects ($P < 0.010$, Figure 4E). As PD-1/PD-L1 blockade can enhance $PD\text{-}1^+$ Treg cell-mediated immunosuppression, Kumagai *et al.* [18] believe that the number of $PD\text{-}1^+$ $CD8^+$ T cells in TME can better

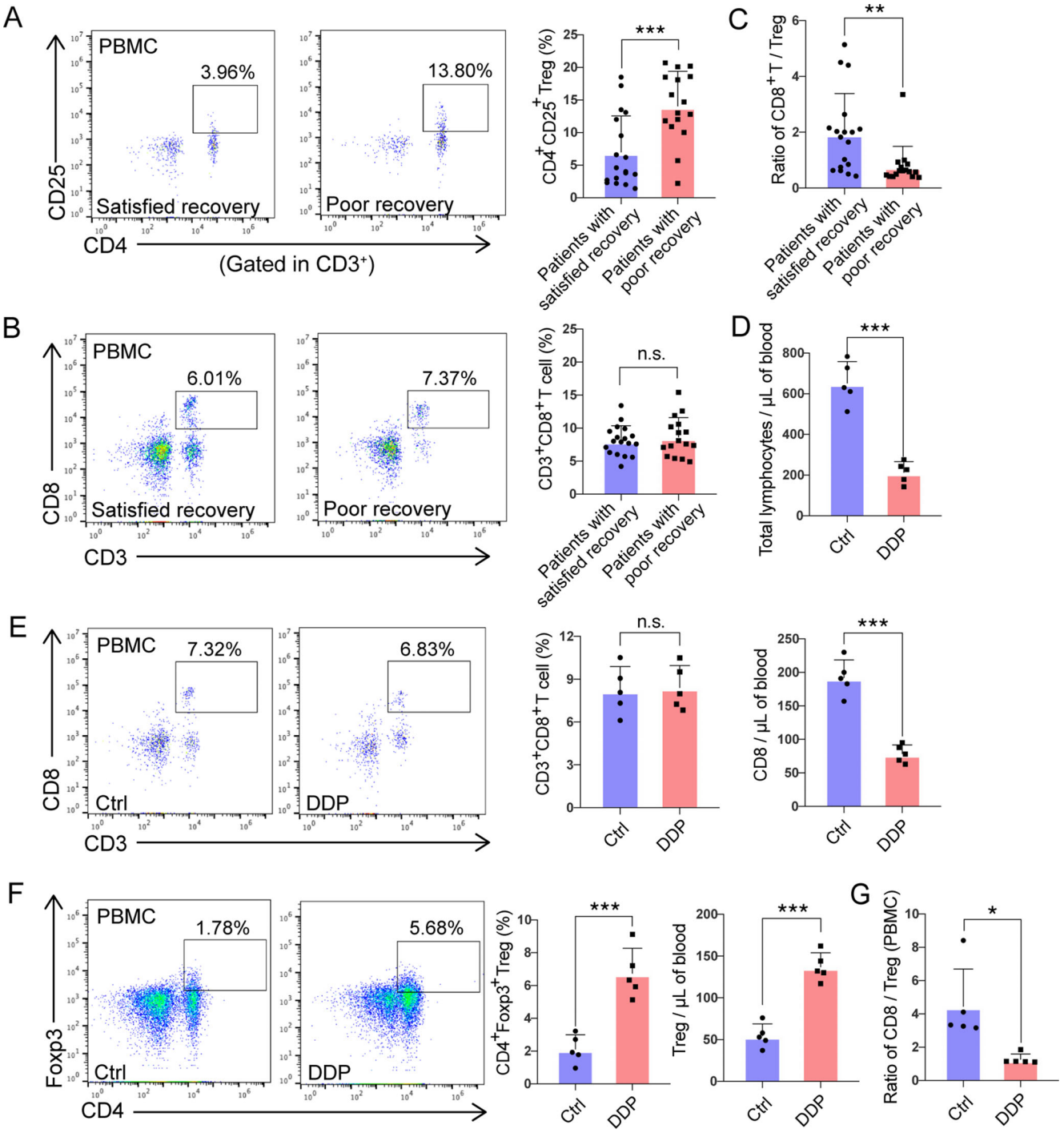


**FIGURE 2** Flow cytometry analysis of peripheral $CD8^+$ T and Treg cells in patients and mouse models lacking lymphocyte recovery. **(A-B)** Flow cytometry analysis of $CD4^+CD25^+$ Tregs (A) and $CD3^+CD8^+$ T cells (B) and from fresh heparinized peripheral blood of patients with satisfactory recovery and poor recovery. $CD4^+CD25^+$ Tregs were gated from $CD3^+$ lymphocytes. **(C)** Comparison of the $CD8^+$ T cell-to-Treg ratio in patients with satisfactory recovery versus poor recovery. **(D)** Absolute counts of total lymphocytes in DDP-treated mice. The mice treated with PBS were used as control (Ctrl). **(E-F)** Percentages, and absolute counts of $CD3^+CD8^+$ T cells (E) and $CD4^+Foxp3^+$ Tregs (F) in the peripheral blood of control and DDP-treated mice. The mice treated with PBS were used as control (Ctrl). Left panel: Flow cytometric plots showing the percentages of $CD3^+CD8^+$ T cells (E) and $CD4^+Foxp3^+$ Tregs (F). Middle and right panel: Columns of percentages (Middle) and absolute counts (Right) of $CD3^+CD8^+$ T cells (E) and $CD4^+Foxp3^+$ Tregs (F). **(G)** The $CD8^+$ T cell/Treg ratio in DDP and control (Ctrl) groups. A-C: satisfied recovery group, $n = 18$; poor recovery group, $n = 16$. D-G: $n = 5$ for each group. For all panels, data are presented as the mean ± SEM for each group. Each point represents an individual animal. *, $P < 0.050$; **, $P < 0.010$; ***, $P < 0.001$; unpaired Student's t-test.

**Abbreviations**: n.s., not significant; DDP, cisplatin; Treg, regulatory T cell; SEM, standard error of the mean

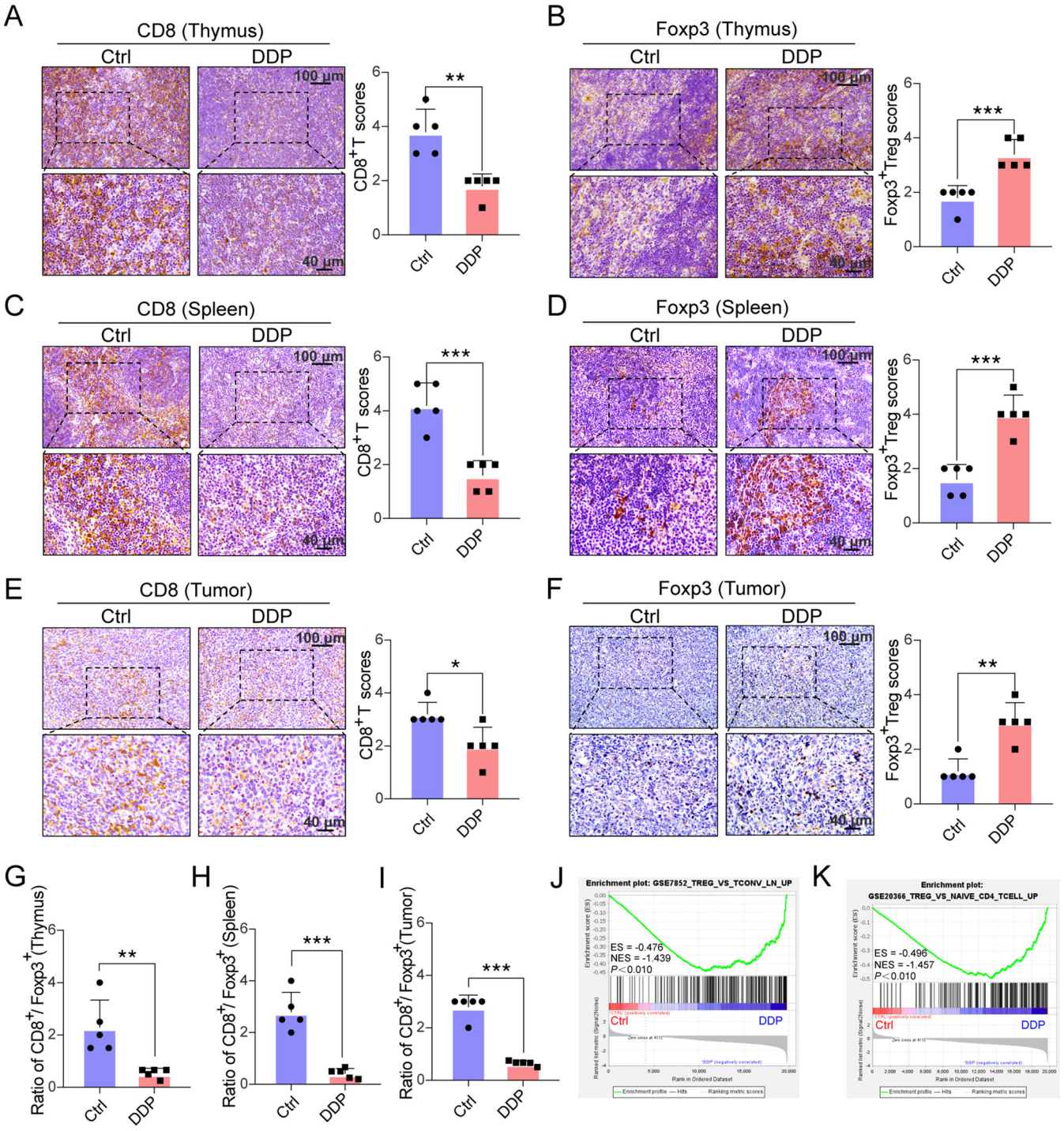


**FIGURE 3** Immunohistochemistry staining of $CD8^+$ T cells and $Foxp3^+$ Tregs in the thymus, spleen and tumor of mice models with impaired lymphocyte recovery. **(A-F)** $CD8^+$ T cells (A, C, E) decreased in specimens of DDP-treated mice, while $Foxp3^+$ Treg cells (B, D, F) increased. Scores for immunohistochemistry staining are presented in bar graphs. Five random fields from each section were counted. Scale bars: 100 $\mu$m, upper panel; 40 $\mu$m, lower panel. **(G-I)** Ratio of $CD8^+/Foxp3^+$ in the thymus (G), spleen (H), and tumor (I). **(J-K)** GSEA plot showing NESs for DDP-induced differentiation of $CD4^+$ T cells to Tregs using RNA-seq data from tumor-infiltrated $CD4^+$ cells. A-I: $n = 5$ for each group. J, K: $n = 2$ for each group. Data are presented as the mean ± SEM for each group. *, $P < 0.050$. **, $P < 0.010$, ***, $P < 0.001$, unpaired Student's t-test.

**Abbreviations**: Treg, regulatory T cell; DDP, cisplatin; GSEA, gene set enrichment analysis; ES, enrichment score; NES, normalized enrichment score

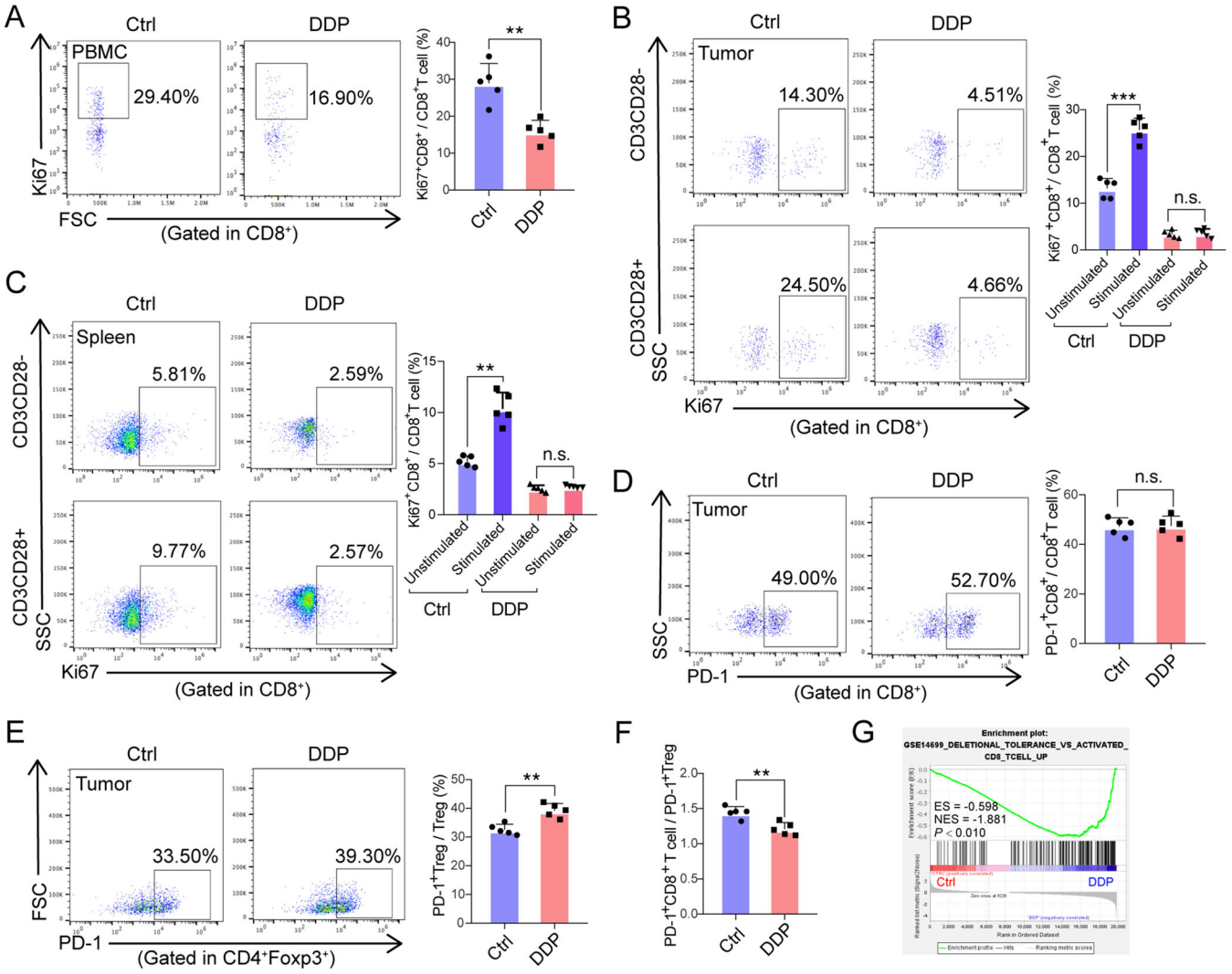


**FIGURE 4** The activation of peripheral, splenic and tumor-infiltrated CD8$^+$ T cells accessed by GSEA and flow cytometry from DDP-treated and control mice. **(A)** Percentage of Ki-67$^+$CD8$^+$ T cells in the peripheral blood are shown for the control (Ctrl) and DDP-treated mice. **(B-C)** Changes in the percentage of Ki-67$^+$CD8$^+$ T cells after CD3 and CD28 (both 1 mg/mL) co-stimulation in tumors (B) and spleens (C) harvested from DDP-treated and control (Ctrl) mice. **(D-E)** Proportions of PD-1$^+$CD8$^+$ T cells and PD-1$^+$CD4$^+$Foxp3$^+$ T cells in tumors harvested from DDP-treated and control (Ctrl) mice. **(F)** The ratio of PD-1$^+$ CD8$^+$ T cells to PD-1$^+$ Treg cells in TME of DDP-treated and control (Ctrl) mice. **(G)** GSEA plot showing NESs for DDP-inhibited activation status, as well as the function of CD8$^+$ T cells using RNA-seq data from tumor infiltrated CD8$^+$ T cells. For all panels, bar graphs represent the means ± SEM for each group. Statistically significant differences are indicated as the results of unpaired Student's t-test (A, D, E, and F) or one-way ANOVA (B and C). A-F: $n = 5$; G: $n = 2$. **, $P < 0.010$; ***, $P < 0.001$.

**Abbreviations**: n.s., not significant; PBMC, peripheral blood mononuclear cell; DDP, cisplatin; SEM, standard error of the mean; FSC, forward scatter; SSC, side scatter; GSEA, gene set enrichment analysis; ES, enrichment score; NES, normalized enrichment score; PD-1, programmed cell death-protein 1

predict the curative effect of anti-PD-1 therapies than PD-1$^+$ Treg cells. This may also be superior to other predictors, such as PD-L1 expression level, or tumor mutational burden (TMB). Thus, we assessed the CD8/Treg ratio of PD-1$^+$ cells in TME and found that the ratio was decreased in response to DDP treatment ($P < 0.010$, Figure 4F). Furthermore, IHC showed similar protein levels of PD-L1 protein expression in the two groups (Figure S1D). We also investigated whether DDP might inhibit CD8$^+$ TIL function using GSEA analysis (GSE14699), which showed that DDP treatment was negatively associated with the activation of CD8$^+$ T cells ($P < 0.010$, Figure 4G). Together, these data suggest that CD8$^+$ T cell function was hampered in the hosts with poor lymphocyte recovery after chemotherapy, possibly causing acquired resistance to PD-1/PD-L1 blockade immunotherapy.

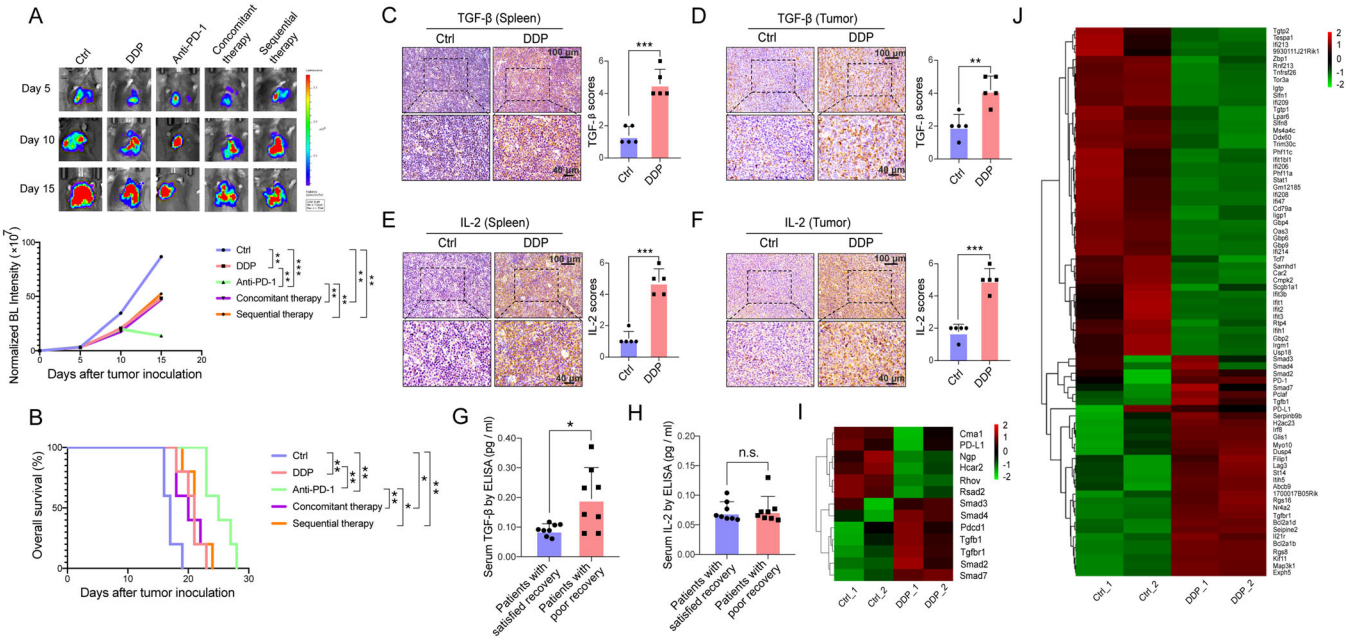


**FIGURE 5** Treatment efficacy of PD-1 blockade immunotherapy was compromised in DDP-treated mice. **(A)** In vivo bioluminescent images and quantification of five groups (control, DDP, anti-PD-1, concurrent DDP + anti-PD-1, sequential DDP + anti-PD-1) at the indicated time points. *P*-value represents a comparison of bioluminescence intensity on the 15th day after injection of luciferase-expressing CMT167 cells into the lungs. **(B)** Kaplan-Meier survival analysis of five groups (control, DDP, anti-PD-1, concurrent DDP + anti-PD-1, sequential DDP + anti-PD-1). **(C-F)** Spleens and tumors of two groups were stained for TGF-$\beta$ (C and D) and IL-2 (E and F). Scale bars: 100 $\mu$m, upper panel; 40 $\mu$m, lower panel. **(G-H)** The serum levels of TGF-$\beta$ (G) and IL-2 (H) in lung cancer patients with or without satisfied recovery were detected by ELISA. **(I-J)** The heatmap shows the gene expression in the TGF-$\beta$ pathway of $CD8^+$ T (I) and Treg cells (J) in control as well as DDP-treated tumors, respectively. As indicated in the scale bar, the values of gene expression are marked in red for high expression and green for low expression. One-way ANOVA statistical tests and log-rank tests were used respectively in A and B. Unpaired t-tests were used to compare two groups (C, D, E, F, G, and H). *, $P < 0.050$; **, $P < 0.010$; ***, $P < 0.001$. A-F: $n = 5$ for each group; G, H: $n = 8$ for each group; I, J: $n = 2$.

**Abbreviations**: n.s., not significant; PD-1, programmed cell death-protein 1; DDP, cisplatin; TGF-$\beta$, transforming growth factor-beta; IL-2, interleukin-2; ELISA, enzyme-linked immunosorbent assay; BL, bioluminescence

## 3.5 | Mice with impaired lymphocyte recovery after chemotherapy are resistant to PD-1 blockade

Since PD-1 blockade can activate $PD\text{-}1^+$ Tregs and induce tumor hyper-progression [19], we hypothesized that Treg activation may compromise the therapeutic efficacy of anti-PD-1 Abs. CMT167 cells, sensitive to PD-1 blockade [20], were stably transfected with firefly luciferase and implanted orthotopically in the lungs. Tumor volumes and luciferase signals were measured every 5 days. As shown in Figures 5A and 5B, single DDP slightly delayed the growth of orthotopic lung tumors and improved mouse survival compared to the control group. Immunotherapy with anti-PD-1 Abs not only slowed tumor growth ($P < 0.001$) but also significantly extended their survival by 7 days (Median survival 17 days vs 24 days, $P < 0.010$). To clarify the timing of combined therapy, the mice were further subdivided into two groups and received immunotherapy concomitant with or sequentially to chemotherapy. However, both groups gained no lasting benefit compared to those treated with DDP alone (Figure 5A and 5B). Taken together, these findings verified that the effectiveness of PD-1 blocking Abs is reduced if lymphocyte recovery is hindered by DDP-based chemotherapy.

## 3.6 | SHR-1701 overcomes the acquired resistance to anti-PD-1 Abs in mice with impaired lymphocyte recovery

To explore the mechanism for accumulation of Tregs in the orthotopic lung cancer models, we analyzed cytokine expression in tumors as well as spleens and found elevated expression of TGF-$\beta$ and IL-2, cytokines related to Treg trafficking (Figure 5C-F). In parallel, serum IL-2 and TGF-$\beta$ were quantified in 8 lung cancer patients with satisfactory lymphocyte recovery and 8 with poor recovery, showing that patients with poor lymphocyte recovery have much higher serum levels of TGF-$\beta$ ($P < 0.050$, Figure 5G),

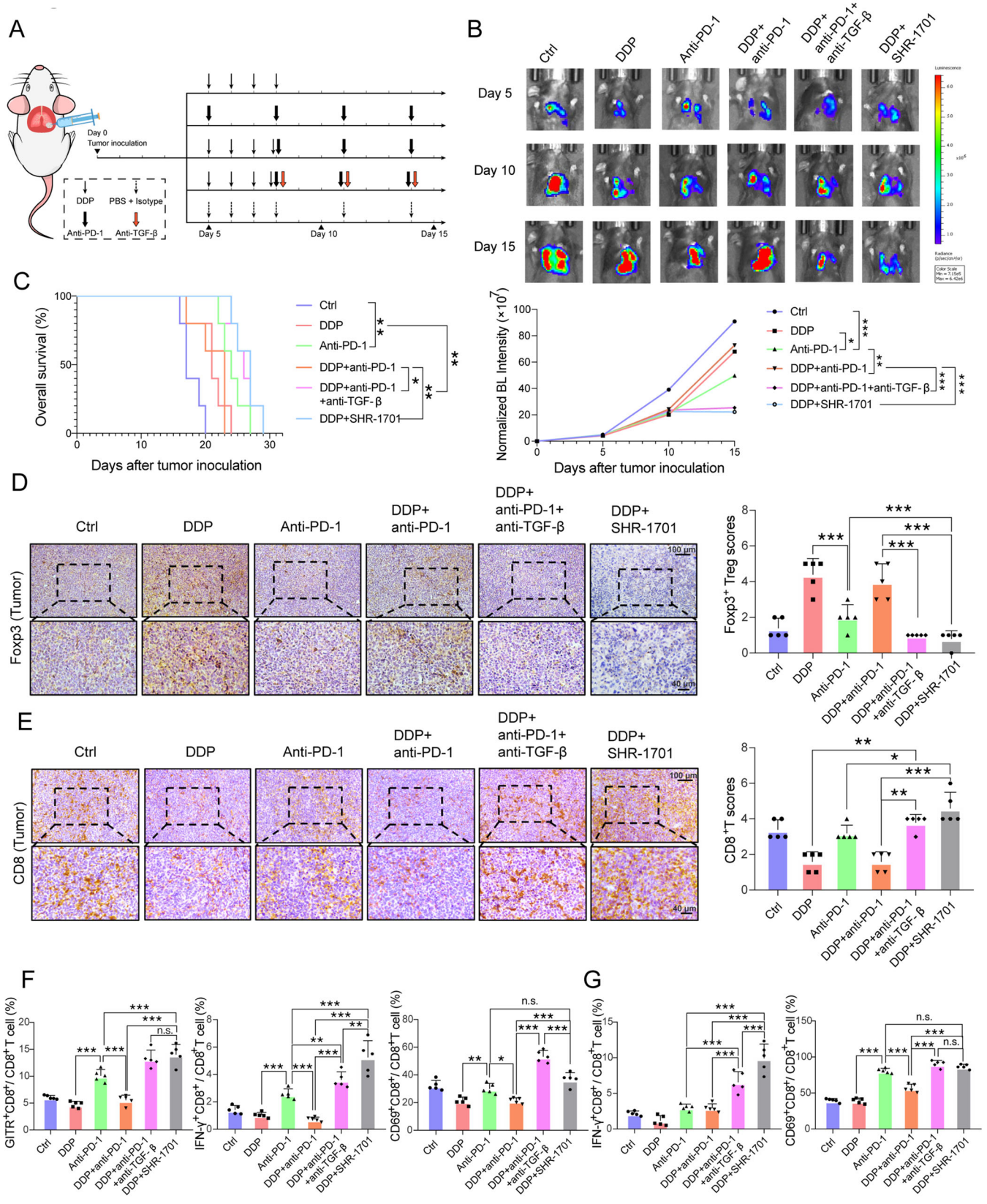


**FIGURE 6** Treatment response of 6 different groups (control, DDP, anti-PD-1, DDP + anti-PD-1, DDP + anti-PD-1 + anti-TGF-$\beta$, DDP + SHR-1701) in an orthotopic mouse model. **(A)** CMT167 cells were transplanted into the lungs of C57BL/6 mice. Follow-up treatment (injected with DDP, anti-PD-1, anti-TGF-$\beta$, SHR-1701, or isotype control antibody) was then performed in six groups as shown. **(B)** Images and quantification of in vivo bioluminescence imaging of the six groups (control, DDP, anti-PD-1, DDP + anti-PD-1, DDP + anti-PD-1 + anti-TGF-$\beta$, DDP + SHR-1701) at the indicated time points. The *P*-value represents a comparison of bioluminescence intensity on the 15th day.

with no significant difference observed between groups regarding IL-2 (Figure 5H). Thus, tumor-infiltrating $CD8^+$ T and Treg cells were sorted from mice and utilized in RNA-seq analysis. Clustering analysis of the RNA-seq data revealed higher expression of entities in the TGF-$\beta$ pathway, both in $CD8^+$ T (Figure 5I) and Treg cells (Figure 5J) isolated from DDP-treated tumors.

TGF-$\beta$ directly promotes the expression of Foxp3 in $CD4^+$ T cells, converting them to a regulatory phenotype [21]. Therefore, we tested the possibility of using TGF-$\beta$ blockade to inhibit Treg cell proliferation and enhance the therapeutic effect of PD-1 inhibitors. Anti-TGF-$\beta$ Abs were administered with anti-PD-1 Abs into tumor-bearing mice (Figure 6A) and bioluminescence signals were recorded 5, 10 and 15 days after CMT167-luc implantation. As shown in Figures 6B and 6C, the bioluminescence intensity of tumors in the control group was the strongest. In the group treated with single DDP, as well as DDP plus anti-PD-1 Ab group, bioluminescence intensity was lower than control but higher than that in the single PD-1 blockade group.

In contrast, the survival of the mice administrated with single DDP and DDP plus anti-PD-1 Abs improved mildly, while single anti-PD-1 Ab administration led to significantly longer survival compared to control mice. M7824, SHR-1701, and YM101 are three humanized bifunctional agents targeting PD-1/PD-L1 and TGF-$\beta$/TGF-$\beta$R simultaneously, among which M7824 and YM101 have been reported to be available in mouse models [22, 23]. For the first time, we confirmed that SHR-1701 efficiently and simultaneously inhibits TGF-$\beta$/TGF-$\beta$R signaling in mouse lung cancer CMT167 cells (Figure S1E and F), suggesting that SHR-1701 might be available in mice models. In vivo experiments showed that SHR-1701, or dual administration of anti-PD-1 and anti-TGF-$\beta$ Abs, induces much stronger tumor regression and significantly longer survival than anti-PD-1 Abs in DDP-treated mice (Figure 6B and 6C).

Based on the above findings, IHC for infiltrating $CD8^+$ T cells and Tregs was performed in tumor tissues and revealed a significant reduction in intra-tumoral Tregs after TGF-$\beta$ blockade or SHR-1701 treatment compared to single PD-1 blockade in DDP-treated mice (Figure 6D). Conversely, an elevation of $CD8^+$ TILs was also observed in triple therapies involving TGF-$\beta$ blockade or doublet therapies involving SHR-1701 (Figure 6E). We then investigated the activation status of $CD8^+$ TILs. In immune responses, GITR is a marker for the identification of Teff cells [24]. Tumor-infiltrating $CD8^+$ T cells from mice receiving triplet therapy or doublet therapy involving SHR-1701 had the highest GITR expression, followed by mice receiving single anti-PD-1 treatment. $CD8^+$ TILs from mice receiving single DDP treatment or DDP plus PD-1 blockade had lower GITR expression than the control group (Figure 6F). After 24 h of co-stimulation with CD3 and CD28, the $CD8^+$IFN-$\gamma^+$, as well as $CD8^+CD69^+$ T cells, were significantly increased in mice receiving triplet therapy or doublet therapy involving SHR-1701, compared with the control mice. $CD8^+$IFN-$\gamma^+$, as well as $CD8^+CD69^+$ T cells, were reduced in mice receiving DDP plus PD-1 blockade, or DDP alone (Figure 6F). Flow cytometry was performed on splenic immune cells. CD69 and IFN-$\gamma$ expression were assessed, with similar results in the $CD8^+$ T cells (Figure 6G). Representative flow cytometric plots of Figures 6F and 6G were shown in Figure S2. These findings collectively indicate that DDP induced an imbalance between $CD8^+$ TILs and Tregs, which could be reversed by TGF-$\beta$/TGF-$\beta$R inhibitors. Dual blockade of both TGF-$\beta$/TGF-$\beta$R and PD-1/PD-L1 achieves better tumor control in mice suffering from DDP-induced poor lymphocyte recovery.

### 3.7 | SHR-1701 treatment increases IFN-$\gamma$ production and Ki-67 expression in peripheral $CD8^+$ T cells in lung cancer patients with poor lymphocyte recovery

Next, we examined whether SHR-1701 could rescue the function of peripheral $CD8^+$ T cells isolated from lung cancer patients suffering from poor lymphocyte recovery. As shown in Figures 7A and 7B, treatment with 10 $\mu$g/mL SHR-1701 significantly upregulated the percentage of IFN-$\gamma^+$ ($P < 0.010$) as well as Ki-$67^+CD8^+$ T cells ($P < 0.050$) after PMA and ionomycin co-stimulation, compared with the anti-PD-1 Abs stimulation group. Moreover, in patients

**(C)** Effect of different treatments (control, DDP, anti-PD-1, DDP + anti-PD-1, DDP + anti-PD-1 + anti-TGF-$\beta$, DDP + SHR-1701) on survival of CMT167 orthotopic tumor-bearing mice. **(D-E)** Representative images of IHC staining for tumor-infiltrating $Foxp3^+$ Treg cells (D) and $CD8^+$ T cells (E). Scale bars: 100 $\mu$m, upper panel; 40 $\mu$m, lower panel. **(F)** Orthotopic tumors were analyzed by flow cytometry for GITR (left panel), IFN-$\gamma$ (middle panel), and CD69 (right panel) expression on $CD8^+$ T cells after stimulation with CD3 and CD28 (both 1 mg/mL) for 48 h. **(G)** IFN-$\gamma$ (left panel) and CD69 (right panel) expression on $CD8^+$ T cells in spleens were analyzed. Bar graphs represent the means ± SEM for each group. B-G: $n = 5$ for each group. One-way ANOVA statistical tests were adopted for more than two groups (B, D, E, F, and G). Log-rank tests were used in C. *, $P < 0.050$; **, $P < 0.010$; ***, $P < 0.001$.

**Abbreviations**: n.s., not significant; PD-1, programmed cell death-protein 1; DDP, cisplatin; TGF-$\beta$, transforming growth factor-beta; Treg, regulatory T cell; IFN-$\gamma$, interferon-$\gamma$; SEM, standard error of the mean; BL, bioluminescence

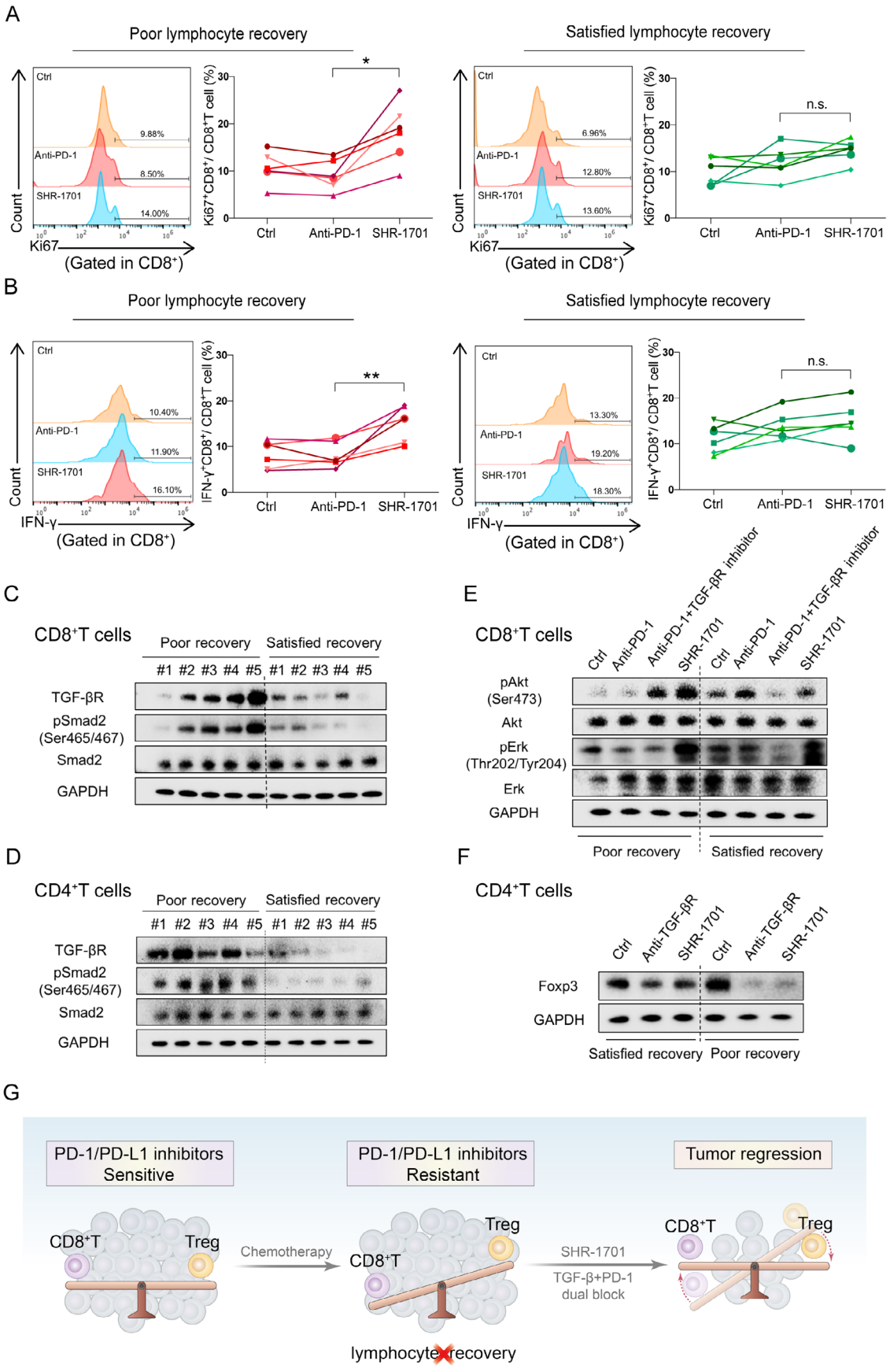


**FIGURE 7** SHR-1701 inhibited TGF-$\beta$ signaling pathway, activated PI3K/Akt/Erk signaling pathway and rescued the anti-tumor function of peripheral CD8$^+$ T cells isolated from lung cancer patients with impaired lymphocyte recovery. **(A-B)** Flow analysis of Ki-67 expression (A) and IFN-$\gamma$ secretion (B) of peripheral CD8$^+$ T cells isolated from patients with satisfied/poor lymphocyte recovery after

with satisfied lymphocyte recovery, anti-PD-1 Abs and SHR-1701 played almost the same role in the activation of T cells, with no statistical differences (Figures 7A and 7B).

Then, we sought to further explore the underlying molecular mechanisms. First, western blotting assay was used to detect TGF-$\beta$ signaling pathway-related proteins, such as TGF-$\beta$R, pSmad2 and Smad2, in peripheral CD8$^+$ T cells to further determine whether the TGF-$\beta$ signaling pathway was activated. The results demonstrated that the expression levels of TGF-$\beta$R and pSmad2 were significantly higher in the patients with poor lymphocyte recovery, indicating a hyper-activation of the TGF-$\beta$ signaling pathway in CD8$^+$ and CD4$^+$ T cells (Figure 7C and 7D). Subsequently, we examined whether the TGF-$\beta$ signaling pathway regulated the activation of the PI3K/Akt/Erk signaling pathway, which was considered to be an essential mechanism for T cell activation. Previous studies have proved that the activation of the PI3K/Akt/Erk pathway in CD8$^+$ T cells led to cell proliferation, release of IFN-$\gamma$ and inhibition of T-regulatory cells [25]. Our western blotting assays showed that PD-1 inhibitors did not elevate the protein level of pAkt and pErk in CD8$^+$ T cells sorted from patients with poor lymphocyte recovery. In contrast, SHR-1701 or combined treatment of TGF-$\beta$R and PD-1 inhibitors seemed to have much more significant effect. However, in patients with satisfied lymphocyte recovery, SHR-1701 or combined treatment of two inhibitors were no better than anti-PD-1 Abs on the activation of pAkt and pErk (Figure 7E). Based on the above results, it was suggested that the over-activation of the TGF-$\beta$ signaling pathway inhibited the PI3K/Akt/Erk activation in CD8$^+$ T cells of patients with impaired lymphocyte recovery. In addition, dual inhibition of both TGF-$\beta$/TGF-$\beta$R and PD-1/PD-L1 could re-activate PI3K/Akt/Erk and then rescue the anti-tumor function of CD8$^+$ T cells. Meanwhile, Foxp3 expression, which indicated Treg differentiation, was detected in CD4$^+$ T cells. The results of western blotting assay showed that SHR-1701 markedly reduced Foxp3 expression in patients with poor lymphocyte recovery but had no effect in those with satisfied lymphocyte recovery (Figure 7F). Since TGF-$\beta$ is one of the key cytokines regulating the development and differentiation of Treg cells [26, 27], it can be inferred that SHR-1701 could inhibit Treg differentiation from CD4$^+$ T cells by blocking TGF-$\beta$/TGF-$\beta$R in patients with poor lymphocyte recovery.

All these data indicate that SHR-1701 might be superior to the first-generation immunotherapeutic agents such as pembrozulimab in lung cancer patients with poor lymphocyte recovery and persistent severe lymphopenia.

## 4 | DISCUSSION

This study demonstrated that lung cancer patients suffering from chemotherapy-related poor lymphocyte recovery had much lower response rates to PD-1/PD-L1 blockade relative to satisfactory lymphocyte recovery patients, suggesting that previous or concurrent chemotherapy may compromise the efficacy of PD-1 blockade in some patients. Similar results were obtained in animal models. While single anti-PD-1 treatment was effective against orthotopic CMT167 lung tumors, it failed to impact those treated together with DDP. IHC and flow cytometry data indicated that the imbalance of CD8$^+$ T/Treg in the tumors may be responsible for the acquired resistance to PD-1/PD-L1 inhibitors. However, SHR-1701 could counteract this imbalance, enhancing the frequency and function of CD8$^+$ TILs, thereby prolonging the survival of mice with disrupted lymphocyte recovery (Figure 7G).

Although huge success has been achieved in the treatment of lung cancer patients, anti-PD-1/PD-L1 Abs are only appropriate for a minority of patients. TMB, as well as PD-L1, are currently used to screen potential beneficiaries of anti-PD-1/PD-L1 Abs. However, there are limited biomarkers that are simple and accurate due to different test procedures, cut-off values, and the lack of sufficient tumor tissue for testing. Hence, there is a need to identify more convenient markers to predict the clinical outcomes of anti-PD-1/PD-L1 Abs. To date, the associations between ALC and the response to immunotherapy remain under debate. Some studies have demonstrated that baseline ALC is significantly correlated with the response to anti-PD-1 in lung cancer patients [28, 29], whereas other studies reported that 80% of the patients with ALC

pre-treatment of SHR-1701 or anti-PD-1 Abs. **(C-D)** Western blotting analysis of the protein levels including TGF-$\beta$R, pSmad2, and total Smad2 in peripheral CD8$^+$(C) or CD4$^+$ (D) T cells from patients with poor/satisfied lymphocyte recovery. **(E)** Western blotting analysis of the activation of pAkt and pErk after treatment of anti-PD-1 blocking Abs/SHR-1701/anti-PD-1 blocking Abs + TGF-$\beta$R inhibitors/PBS in peripheral CD8$^+$ T cells sorted from patients. **(F)** Western blotting analysis of the expression of Foxp3 after treatment of SHR-1701/TGF-$\beta$R inhibitors/PBS in peripheral CD4$^+$ T cells sorted from patients. (G) SHR-1701 reverses the tumor's response to PD-1 blockade immunotherapy, from resistant to sensitive, by regulating the balance between CD8$^+$ T cells and Tregs. A-B: $n = 6$ for each group. C-D: $n = 5$ for each group. E, F: The examination was repeated in 3 patients with poor recovery and 3 patients with satisfied recovery. One-way ANOVA statistical tests were adopted for A and B. *, $P < 0.050$; **, $P < 0.010$.

**Abbreviations**: n.s., not significant; PD-1, programmed cell death-protein 1; TGF-$\beta$R, transforming growth factor-beta receptor; TGF-$\beta$, transforming growth factor-beta; IFN-$\gamma$, interferon-$\gamma$

lower than $0.5*10^9$/L still had their disease under control [30]. No prior study investigated lymphocyte recovery in patients undergoing PD-1/PD-L1 blockade immunotherapy. The present study demonstrated that lymphocyte recovery, a hematologic feature easy to detect, was associated with response to immunotherapy while temporary and reversible lymphopenia did not reduce the efficacy of cancer immunotherapies. Lymphocyte recovery must be considered, especially in heavily pre-treated patients, for whom the prognostic value of traditional biomarkers such as PD-L1 expression seems to be less significant [31].

Currently, the efficacy of combined immunotherapy and chemotherapy has been demonstrated in many published clinical trials. Combined immunotherapy and chemotherapy have a synergistic effect on survival compared with chemotherapy alone [32–35]. However, the stratification and subgroup analyses for lymphocyte recovery have been long neglected and no study has been reported on it. Among some patients, chemotherapy was well-tolerated, and their peripheral lymphocytes could recover quickly in three weeks. For these patients, combined therapies should be considered. However, our study focused on patients whose lymphocyte recovery was fragile and easily been impaired by tumors or anti-tumor chemotherapy. In our study, an animal model of poor lymphocyte recovery was successfully established, based on which we found that Treg/$CD8^+$T cells were reversed in the lymphoid organs and tumors. We also verified that the immunosuppressive state was not induced by the elevation of PD-1/PD-L1. Besides, we proposed that chemotherapy activated the TGF-$\beta$ signaling pathway, which then promoted Treg differentiation and inhibited the proliferation of $CD8^+$ T cells, making PD-1 blockade ineffective. In addition, our findings indicated that patients with poor lymphocyte recovery were in a special immune state, requiring close attention to their medication safety. Clinical trials specifically dedicated to these patients, or larger studies involving subgroup analyses for lymphocyte recovery are necessary to be further investigated in the future.

Moreover, to counteract the relatively low response, second-generation bifunctional drugs targeting PD-1/PD-L1 and TGF-$\beta$/TGF-$\beta$R have been developed, such as M7824, SHR-1701, and YM101, of which M7824 and SHR-1701 have been already used in clinical trials [36]. Thus, the following question arises: which is better for a certain patient? According to our results, lymphocyte recovery could allow early identification of non-responders to traditional PD-1/PD-L1 blockers and timely use of bifunctional drugs such as SHR-1701. Thus, this is the first report that might help doctors to match the first or second generation of drugs to patients.

To date, no prior study has elucidated how chemotherapy alters the homeostatic lymphocyte subsets within peripheral blood of cancer patients. Previous studies found a depletion of Tregs during cycles of chemotherapy [37], however, our study identified a specific patient subpopulation (with poor lymphocyte recovery), in which chemotherapy can accumulate Tregs and deplete $CD8^+$ T cells . Moreover, TGF-$\beta$ was elevated both in the serum and TME. As reported by in vivo studies, TGF-$\beta$ blockade by anti-TGF-$\beta$ Abs or SHR-1701 increases the ratio of $CD8^+$ T to Treg cells, and cytokine production in $CD8^+$ T cells, prolonging the survival of mice with lung cancer. M7824 and YM101 have been proved to efficiently bind PD-L1, trap TGF-$\beta$ and suppress tumor growth in syngeneic mouse models, although they are humanized Abs [22, 23]. Here for the first time, our western blotting analysis in murine CMT167 cells showed that SHR-1701 successfully blocked the downstream pSmad2 signaling pathway of TGF-$\beta$/TGF-$\beta$R and rescued the downstream pAkt pathway of PD-1/PD-L1. Moreover, SHR-1701 prolonged survival and endowed long-lasting immunity against tumors among C57BL/6 mice bearing lung cancer CMT167 cells. Collectively, this indicated that blockade of both PD-L1 and TGF-$\beta$R pathways promotes potent and predominant protections from tumors compared to PD-1/PD-L1 targeting monotherapy in tumor bearers suffering from a chemotherapy-induced immune disorder.

Admittedly, as with many preclinical mouse models, the CMT167 lung tumor model showing $\geq$ 50% efficacy to anti-PD-1 therapy does not truly mirror the less than 20% clinical response observed in humans. In addition, animal experimentation does not offer safety assurances for patients. Therefore, our primary focus was to gain insight into how previous therapies may dictate the differential response between responders and non-responders and, in turn, to explore interventions that can transform non-responders into responders. Further clinical studies are required.

In conclusion, the present results indicate that the therapeutic efficacy of PD-1/PD-L1 inhibitors can be greatly reduced in pre-treated lung cancer patients with disrupted lymphocyte recovery. Compared to the first-generation drugs, combination with TGF-$\beta$/TGF-$\beta$R inhibitors or administration of bifunctional drugs, such as SHR-1701, can reverse the imbalance of $CD8^+$ T/Treg cells and elicit predominant protection against tumors.

## DECLARATIONS

### ETHICS APPROVAL AND CONSENT TO PARTICIPATE

This study was approved by the Medical Ethical Committee of Qilu Hospital affiliated to Shandong University (KYLL-2019-2-004 and KYLL-2020-045). All samples

were obtained with informed consent in accordance with the Declaration of Helsinki. All animal experimental procedures were performed in accordance with the protocols approved by the Institutional Animal Care and Use Committee (IACUC) and Research Advisory Committee of Shandong University.

## CONSENT FOR PUBLICATION

Not applicable.

## AVAILABILITY OF DATA AND MATERIALS

The datasets used and analyzed in this study are available from the corresponding author on reasonable request.

## COMPETING INTERESTS

The authors declare that they have no competing interests.

## ACKNOWLEDGEMENTS

The study was supported by funding from the Shandong Provincial Natural Science Foundation (ZR201807080057), the National Key Research and Development Projects of China (2018YFC1312201), Cancer Institute and Hospital, Chinese Academy of Medical Sciences (2019RU071), the Academic Promotion Program of Shandong First Medical University (2019ZL002), and the National Natural Science Foundation of China (81803096, 81972863, 81627901, and 82030082).

## AUTHORS' CONTRIBUTIONS

YL and JMY conceived and designed the project. BC, YL, PXC, KKD, and TL performed the experiments. BC, YL and XFG analyzed the data. YL, BC, WQ, CHM, and JXJ wrote the manuscript. JW, JMY and YL provided the reagents and materials. XM, JMY, YL and JW supervised the study. All authors read and approved the final manuscript.

## ORCID

*Jinming Yu* https://orcid.org/0000-0001-5933-9912
*Yuan Liu* https://orcid.org/0000-0002-4425-2213

## REFERENCES

1. Siegel RL, Miller KD. A Jemal Cancer statistics, 2019. CA Cancer J Clin. 2019;69(1):7–34.
2. Garon EB, Rizvi NA, Hui R, Leighl N, Balmanoukian AS, Eder JP, et al. Pembrolizumab for the treatment of non-small-cell lung cancer. N Engl J Med. 2015;372(21):2018–28.
3. Paz-Ares L, Kim TM, Vicente D, Felip E, Lee DH, Lee KH, et al. Bintrafusp alfa, a bifunctional fusion protein targeting TGF-$\beta$ and PD-L1, in second-line treatment of patients with NSCLC: results from an expansion cohort of a phase 1 trial. J Thorac Oncol. 2020;15(7):1210–22.
4. Merck Announces Update on the INTR@PID Clinical Program Including Lung 037 Study. Available from: https://www.merckgroup.com/en/news/bintrafusp-alfa-037-update-20-01-2021.html.
5. McCoy MJ, Lake RA, van der Most RG, Dick IM. AK Nowak Post-chemotherapy T-cell recovery is a marker of improved survival in patients with advanced thoracic malignancies. Br J Cancer. 2012;107(7):1107–15.
6. Lee BM, Byun HK. J Seong Significance of lymphocyte recovery from treatment-related lymphopenia in locally advanced pancreatic cancer. Radiother Oncol. 2020;151:82–7.
7. Wang LX, Shu S, Plautz GE. Host lymphodepletion augments T cell adoptive immunotherapy through enhanced intratumoral proliferation of effector cells. Cancer Res. 2005;65(20):9547–54.
8. Grossman SA, Ellsworth S, Campian J, Wild AT, Herman JM, Laheru D, et al. Survival in Patients With Severe Lymphopenia Following Treatment With Radiation and Chemotherapy for Newly Diagnosed Solid Tumors. J Natl Compr Canc Netw. 2015;13(10):1225–31.
9. Diem S, Schmid S, Krapf M, Flatz L, Born D, Jochum W, et al. Neutrophil-to-Lymphocyte ratio (NLR) and Platelet-to-Lymphocyte ratio (PLR) as prognostic markers in patients with non-small cell lung cancer (NSCLC) treated with nivolumab. Lung Cancer. 2017;111:176–81.
10. Russo A, Russano M, Franchina T, Migliorino MR, Aprile G, Mansueto G, et al. Neutrophil-to-Lymphocyte Ratio (NLR), Platelet-to-Lymphocyte Ratio (PLR), and Outcomes with nivolumab in pretreated Non-Small Cell Lung Cancer (NSCLC): a large retrospective multicenter study. Adv Ther. 2020;37(3):1145–55.
11. Sprent J, Surh CD. Normal T cell homeostasis: the conversion of naive cells into memory-phenotype cells. Nat Immunol. 2011;12(6):478–84.
12. Eldershaw S, Verma K, Croft W, Rai T, Kinsella F, Stephens C, et al. Lymphopenia-induced lymphoproliferation drives activation of naive T cells and expansion of regulatory populations. iScience. 2021;24(3):102164.
13. Zhang N, Bevan MJ. TGF-$\beta$ signaling to T cells inhibits autoimmunity during lymphopenia-driven proliferation. Nat Immunol. 2012;13(7):667–73.
14. Ciurea SO, Mulanovich V, Jiang Y, Bassett R, Rondon G, McMannis J, et al. Lymphocyte recovery predicts outcomes in cord blood and T cell-depleted haploidentical stem cell transplantation. Biol Blood Marrow Transplant. 2011;17(8):1169–75.
15. Ji J, Ding K, Luo T, Zhang X, Chen A, Zhang D, et al. TRIM22 activates NF-$\kappa$B signaling in glioblastoma by accelerating the degradation of I$\kappa$B$\alpha$. Cell Death Differ. 2021;28(1):367–81.
16. Kumawat AK, Strid H, Elgbratt K, Tysk C, Bohr J, Hultgren E. Hornquist Microscopic colitis patients have increased proportions of Ki67(+) proliferating and CD45RO(+) active/memory CD8(+) and CD4(+)8(+) mucosal T cells. J Crohns Colitis. 2013;7(9):694–705.
17. Huang AC, Postow MA, Orlowski RJ, Mick R, Bengsch B, Manne S, et al. T-cell invigoration to tumour burden ratio associated with anti-PD-1 response. Nature. 2017;545(7652):60–5.
18. Kumagai S, Togashi Y, Kamada T, Sugiyama E, Nishinakamura H, Takeuchi Y, et al. The PD-1 expression balance between effector and regulatory T cells predicts the clinical efficacy of PD-1 blockade therapies. Nat Immunol. 2020;21(11):1346–58.
19. Kamada T, Togashi Y, Tay C, Ha D, Sasaki A, Nakamura Y, et al. PD-1(+) regulatory T cells amplified by PD-1 blockade

promote hyperprogression of cancer. Proc Natl Acad Sci U S A. 2019;116(20):9999–10008.
20. Li HY, McSharry M, Bullock B, Nguyen TT, Kwak J, Poczobutt JM, et al. The Tumor Microenvironment Regulates Sensitivity of Murine Lung Tumors to PD-1/PD-L1 Antibody Blockade. Cancer Immunol Res. 2017;5(9):767–77.
21. Smith AL, Robin TP. Ford HL. Molecular pathways: targeting the TGF-beta pathway for cancer therapy. Clin Cancer Res. 2012;18(17):4514–21.
22. Lan Y, Zhang D, Xu C, Hance KW, Marelli B, Qi J, et al. Enhanced preclinical antitumor activity of M7824, a bifunctional fusion protein simultaneously targeting PD-L1 and TGF-$\beta$. Sci Transl Med. 2018;10(424):eaan5488.
23. Yi M, Zhang J, Li A, Niu M, Yan Y, Jiao Y, et al. The construction, expression, and enhanced anti-tumor activity of YM101: a bispecific antibody simultaneously targeting TGF-$\beta$ and PD-L1. J Hematol Oncol. 2021;14(1):27.
24. Riccardi C, Ronchetti S, Nocentini G. Glucocorticoid-induced TNFR-related gene (GITR) as a therapeutic target for immunotherapy. Expert Opin Ther Targets. 2018;22(9):783–97.
25. Rogel A, Willoughby JE, Buchan SL, Leonard HJ, Thirdborough SM, Al-Shamkhani A. Akt signaling is critical for memory CD8(+) T-cell development and tumor immune surveillance. Proc Natl Acad Sci U S A. 2017;114(7):E1178–87.
26. Brown H, Esterhazy D Paying a price twice: Dose-dependent effects of treg cell-derived TGF- beta on tolerance. Immunity. 2020;53(6):1128–30.
27. Ansa-Addo EA, Zhang Y, Yang Y, Hussey GS, Howley BV, Salem M, et al. Membrane-organizing protein moesin controls Treg differentiation and antitumor immunity via TGF-beta signaling. J Clin Invest. 2017;127(4):1321–37.
28. Soyano AE, Dholaria B, Marin-Acevedo JA, Diehl N, Hodge D, Luo Y, et al. Peripheral blood biomarkers correlate with outcomes in advanced non-small cell lung Cancer patients treated with anti-PD-1 antibodies. J Immunother Cancer. 2018;6(1):129.
29. Karantanos T, Karanika S, Seth B, Gignac G. The absolute lymphocyte count can predict the overall survival of patients with non-small cell lung cancer on nivolumab: a clinical study. Clin Transl Oncol. 2019;21(2):206–12.
30. Sun R, Champiat S, Dercle L, Aspeslagh S, Castanon E, Limkin EJ, et al. Baseline lymphopenia should not be used as exclusion criteria in early clinical trials investigating immune checkpoint blockers (PD-1/PD-L1 inhibitors). Eur J Cancer. 2017;84:202–11.
31. Lang D, Huemer F, Rinnerthaler G, Horner A, Wass R, Brehm E, et al. Therapy line and associated predictors of response to PD-1/PD-L1-inhibitor monotherapy in advanced non-small-cell lung cancer: A retrospective Bi-centric cohort study. Target Oncol. 2019;14(6):707–17.
32. Leonetti A, Wever B, Mazzaschi G, Assaraf YG, Rolfo C, Quaini F, et al. Molecular basis and rationale for combining immune checkpoint inhibitors with chemotherapy in non-small cell lung cancer. Drug Resist Updat. 2019;46:100644.
33. Wang X, Niu X, An N, Sun Y, Chen Z. Comparative Efficacy and Safety of Immunotherapy Alone and in Combination With Chemotherapy for Advanced Non-small Cell Lung Cancer. Front Oncol. 2021;11:611012.
34. Wang C, Qiao W, Jiang Y, Zhu M, Shao J, Wang T, et al. The landscape of immune checkpoint inhibitor plus chemotherapy versus immunotherapy for advanced non-small-cell lung cancer: A systematic review and meta-analysis. J Cell Physiol. 2020;235(5):4913–27.
35. Yang ZR, Liu MN, Yu JH, Yang YH, Chen TX, Han YC, et al. Treatment of stage III non-small cell lung cancer in the era of immunotherapy: pathological complete response to neoadjuvant pembrolizumab and chemotherapy. Transl Lung Cancer Res. 2020;9(5):2059–73.
36. Strauss J, Heery CR, Schlom J, Madan RA, Cao L, Kang Z, et al. Phase I Trial of M7824 (MSB0011359C), a Bifunctional Fusion Protein Targeting PD-L1 and TGF$\beta$, in Advanced Solid Tumors. Clin Cancer Res. 2018;24(6):1287–95.
37. Wu L, Yun Z, Tagawa T, Rey-McIntyre K, Anraku M, de Perrot M. Tumor cell repopulation between cycles of chemotherapy is inhibited by regulatory T-cell depletion in a murine mesothelioma model. J Thorac Oncol. 2011;6(9):1578–86.

## SUPPORTING INFORMATION

Additional supporting information may be found in the online version of the article at the publisher's website.

**How to cite this article:** Cheng Bo, Ding K, Chen P, Ji J, Luo T, Guo X, et al. Anti-PD-L1/TGF-$\beta$R fusion protein (SHR-1701) overcomes disrupted lymphocyte recovery-induced resistance to PD-1/PD-L1 inhibitors in lung cancer. Cancer Commun. 2022;42:17–36.
https://doi.org/10.1002/cac2.12244